FISEVIER

Contents lists available at ScienceDirect

Materials Science & Engineering A

journal homepage: www.elsevier.com/locate/msea



The effect of heat treatment on precipitation in the Cu-Ni-Al alloy Hiduron® 130



Katerina A. Christofidou^{a,*,1}, K. Jennifer Robinson^a, Paul M. Mignanelli^a, Ed J. Pickering^b, Nicholas G. Jones^a, Howard J. Stone^a

- ^a Department of Materials Science and Metallurgy, University of Cambridge, 27 Charles Babbage Road, Cambridge CB3 0FS, UK
- ^b School of Materials, The University of Manchester, Manchester M13 9PL, UK

ARTICLE INFO

Keywords: Copper alloys L12 phase Microstructure SEM TEM XRD

ABSTRACT

Cupronickel alloys, reinforced by $\rm L1_2$ precipitates, offer a high strength, corrosion resistant and anti-bio fouling material for marine engineering applications. These alloys exhibit complex precipitate nucleation and growth mechanisms that must be fully understood in order to optimise the mechanical properties. In this work, the microstructural characteristics of the Cu-Ni-Al based alloy, Hiduron® 130, have been assessed in the as-received condition and following 100-h thermal exposures at 500, 600, 700 and 900 °C and after a two-stage exposure at 900 °C for 100 h followed by 500 °C for 100 h. The $\rm L1_2$ phase was observed to precipitate both discontinuously and continuously and its subsequent coarsening was characterised alongside measurements of the lattice misfit. The hardness of the alloy was found to decrease with increasing exposure temperature up to the $\rm L1_2$ solvus and correlated with the evolution of the $\rm L1_2$ precipitates, the alloy grain size and the fraction of the discontinuously formed $\rm L1_2$ phase.

1. Introduction

Precipitate hardened cupronickel alloys possess a combination of properties that makes them ideally suited for highly loaded components in marine engineering. The alloys benefit from superior mechanical properties than binary cupronickel alloys, whilst retaining excellent corrosion resistance in aqueous environments, a low susceptibility to hydrogen embrittlement and stress corrosion cracking, and good antibiofouling properties [1]. Furthermore, recent research has identified Cu-Ni-Al alloys as possible replacements for precipitate hardened Cu-Be alloys used in electronics applications on account of the toxicity of Be [2–4].

High strength cupronickel alloys may be realised through Al additions to Cu-Ni binary alloys, which provide age hardening through the formation of L1 $_2$ (Strukterbericht notation) precipitates, analogous to the well-known γ' particles found in Ni-based superalloys [5]. Precipitation of the L1 $_2$ phase in cupronickel alloys provides a large improvement in the mechanical properties, not only through conventional precipitation hardening mechanisms, but also as a result of the ordered nature of the precipitates and their crystallographic similarity to the A1 matrix in which they reside. The passage of a/2 $\langle\bar{1}10\rangle$ dislocations from the A1 matrix into the ordered L1 $_2$ phase encounters

increased resistance, due to the energy penalty associated with the formation of an anti-phase boundary created in the $L1_2$ structure, which can only be reduced by the passage of a second dislocation through the precipitate [6-8].

Previous studies have reported on the microstructural characteristics and $\rm L1_2$ precipitation behavior of Cu-Ni-Al alloys [4,9–12], the effect of thermomechanical treatments on the alloy properties and microstructure [2,10,13,14] as well as the effect of additional alloying elements [2,10,15]. Precipitation of the $\rm L1_2$ phase in Cu-Ni-Al alloys occurs through both continuous and discontinuous processes, whereas, for alloys with high concentrations of Al, the B2 – NiAl phase may also precipitate [5,9–11,13,14]. The discontinuous precipitation of the $\rm L1_2$ phase, as well as the formation of the B2 phase, will result in the weakening of the alloy through the consumption of Al, leading to a reduction in the volume fraction of the continuously precipitated $\rm L1_2$ phase.

Several compositions of Cu-Ni-Al-based alloys have been studied with the aim of determining the optimal thermomechanical processing route, and in particular, the optimum L1 $_2$ precipitate size required to maximise the mechanical properties [11,12,14,16]. Whilst these studies presented a very thorough characterisation of the evolution of the continuous distributions of the L1 $_2$ phase at ~500 °C with varying

^{*} Corresponding author.

E-mail address: kc424@cam.ac.uk (K.A. Christofidou).

¹ ORCID: 0000-0002-8064-5874.

Table 1The chemical composition of Hiduron® 130, as provided by Langley Alloys.

Element	Cu	Ni	Al	Fe	Mn	Trace elements
wt%	81.7	14.4	2.7	0.8	0.3	0.1
at%	77.9	14.8	6.0	0.9	0.3	0.1

exposure lengths, the effect of different exposure temperatures is not well understood. In addition, although discontinuously precipitated colonies of the $\rm L1_2$ phase have been reported to occur, the driving force for this precipitation phenomenon is not well documented.

Consequently, this work aims to contribute towards an improved understanding of both the continuous and discontinuous precipitation behavior in the commercially available Cu-Ni-Al alloy, Hiduron* 130. The distribution of the L1 $_2$ precipitates and the lattice misfit in the alloy were studied with respect to the exposure temperature. In addition, the hardness of the material following ageing was measured and correlated to the microstructural observations.

2. Experimental

The chemical composition of Hiduron® 130, as provided by Langley Alloys, is shown in Table 1. The liquidus, solidus and L1 $_2$ solvus temperatures were determined using differential scanning calorimetry (DSC), with a 5 mm diameter disc cut from a 1 mm thick slice of the asreceived material. Calorimetric data was acquired using a Netzsch 404 calorimeter with an argon atmosphere and a heating/cooling rate of $10\ ^{\circ}\mathrm{C}\ \mathrm{min}^{-1}$. Heat treatment of the alloy was performed in argon-backfilled quartz ampoules and exposed for 100 h at temperatures of 500, 600, 700 and 900 °C. An additional two-stage exposure at 900 °C for 100 and 500 °C for 100 h was also performed. All samples were air cooled from the exposure temperature.

Samples for scanning electron microscopy (SEM) were prepared following standard metallographic preparation techniques. Final polishing of the samples was achieved using a neutral solution of $0.06~\mu m$ colloidal silica in H_2O_2 . An FEI Nova NanoSEM 450 equipped with a Bruker XFlash 6 solid-state energy dispersive X-ray spectroscopy (EDX) detector was used for the microstructural analysis.

Samples for transmission electron microscopy (TEM) analysis, were prepared as discs 3 mm in diameter and 100 μm thick from as-received material before thinning using a Gatan 691 Precision Ion Polishing System. Final polishing was performed using a 5 eV argon beam for 30 min, followed by a 1 eV beam for 30 min. TEM investigations were carried out on an FEI Tecnai Osiris microscope operated at 200 kV and equipped with FEI Super-X EDX detectors. An average particle size distribution was obtained from the microstructural images using the ImageJ software package.

X-ray diffraction (XRD) patterns were collected from 20° to $120^{\circ}~2\theta$

on a Bruker D8 diffractometer using Ni-filtered Cu-K α radiation. To obtain the lattice parameters of the phases present in the structure, the diffraction spectra were fitted using the Pawley method [17] in the TOPAS-academic software package. The lattice misfit (δ) between the Cu-rich A1 matrix and the L1₂ precipitates was calculated from the lattice parameters using Eq. (1).

$$\delta = 2 \left[\frac{\alpha_{Ll_2} - \alpha_{A1}}{\alpha_{Ll_2} + \alpha_{A1}} \right] \tag{1}$$

The hardness of the material in each condition was evaluated using a Vickers hardness indenter operated with an applied load of 20 kg and a dwell time of 30 s. Ten measurements were obtained from each sample, which were averaged to provide a mean value of hardness.

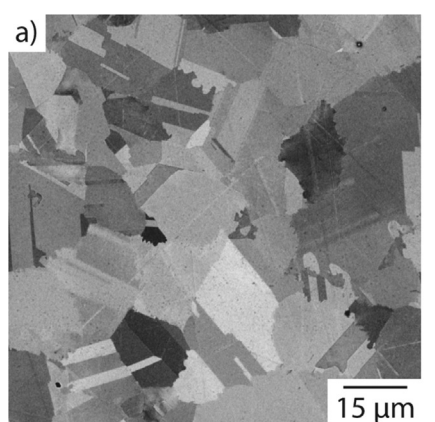
3. Results

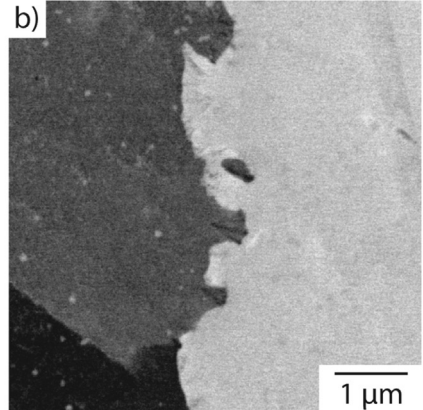
3.1. Microstructural characterisation of as-received Hiduron® 130

Understanding the microstructure of the as-received material was vitally important for tracking the evolution of the alloy microstructure following the thermal exposures. Fig. 1 presents backscattered electron images of the key features observed in the alloy in the as-received state. The grain structure of the material is shown in Fig. 1a, from which the average grain size was found to be ${\sim}14\pm5\,\mu\text{m}$ in diameter. Closer examination also revealed regions of discontinuous precipitation and the formation of discrete dark particles at the grain boundaries, as shown in Fig. 1b and c. However, the L12 particles were not observed at this length scale, hence, TEM-based techniques were utilised to confirm the presence of nanosized L12 precipitates.

Fig. 2 presents the collective results from the TEM analyses; Fig. 2a shows a high angle annular dark field (HAADF) scanning transmission electron microscopy (STEM) image of the bulk material, and is accompanied by EDX maps of the key elements in the alloy: Ni, Fe, Al and Cu, shown in Fig. 2b-e respectively. The EDX results indicated that Cu was the principal constituent of the A1 matrix whilst Ni and Al preferentially partitioned to the L12 precipitates. Fe also displayed preferential partitioning towards the L1₂ phase, but to a lesser extent than Ni and Al. Fig. 2f shows the electron diffraction pattern from a typical region of the material in which fundamental reflections from the A1 matrix were observed, along with superlattice reflections indicative of the presence of the L12 phase. A dark field image obtained from the (100) superlattice reflection is included in Fig. 2f in which the L1₂ precipitates may be clearly discerned. Using data from both the STEM and dark field images, the L12 phase was found to form in a spherical morphology with an average diameter of 18 ± 6 nm.

As stated previously, in addition to L1₂ precipitation, the formation of discrete grain boundary particles and discontinuously precipitated colonies were observed in the alloy. HAADF STEM images and EDX





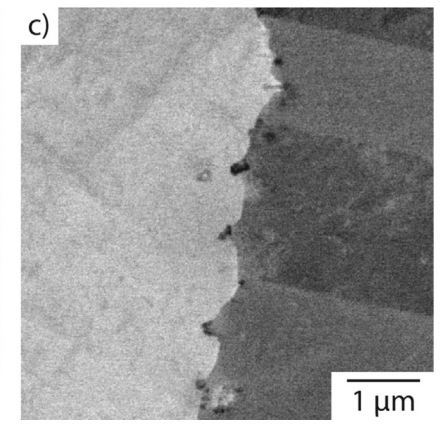


Fig. 1. Back scattered electron images of Hiduron® 130 in the as-received state. a) Grain structure, b) discontinuously precipitated colonies and c) grain boundary pinning particles.

Download English Version:

https://daneshyari.com/en/article/5455803

Download Persian Version:

https://daneshyari.com/article/5455803

Daneshyari.com